8 Tabaru A, Narita R, Hiura M, Abe S, Otsuki M. Efficacy of short-term interferon therapy for patients infected with hepatitis C virus genotype 2a. *Am J Gastroenterol* 2005; **100**: 862–7.
9 Kawamura Y, Arase Y, Ikeda K *et al.* The efficacy of short-term interferon-beta therapy for chronic hepatitis C patients with low virus load. *Intern Med* 2008; **47**: 355–60.
10 Zeuzem S, Buti M, Ferenci P *et al.* Efficacy of 24 weeks treatment with peginterferon alfa-2b plus ribavirin in patients with chronic hepatitis C infected with genotype 1 and low pretreatment viremia. *J Hepatol* 2006; **44**: 97–103.
11 Arase Y, Suzuki F, Akuta N *et al.* Combination therapy of peginterferon and ribavirin for chronic hepatitis C patients with genotype 1b and low-virus load. *Intern Med* 2009; **48**: 253–8.
12 Okanoue T, Itoh Y, Hashimoto H *et al.* Predictive values of amino acid sequences of the core and NS5A regions in antiviral therapy for hepatitis C: a Japanese multi-center study. *J Gastroenterol* 2009; **44**: 952–63.
13 Tanaka Y, Nishida N, Sugiyama M *et al.* Genome-wide association of IL28B with response to pegylated interferon-alpha and ribavirin therapy for chronic hepatitis C. *Nat Genet* 2009; **41**: 1105–9.
14 Akuta N, Suzuki F, Hirakawa M *et al.* Amino acid substitution in hepatitis C virus core region and genetic variation near the interleukin 28B gene predict viral response to telaprevir with peginterferon and ribavirin. *Hepatology* 2010; **52**: 421–9.
15 Hayashi K, Katano Y, Ishigami M *et al.* Mutations in the core and NS5A region of hepatitis C virus genotype 1b and correlation with response to pegylated-interferon-alpha 2b and ribavirin combination therapy. *J Viral Hepat* 2011; **18**: 280–6.
16 Hayashi K, Katano Y, Honda T *et al.* Association of interleukin 28B and mutations in the core and NS5A region of hepatitis C virus with response to peg-interferon and ribavirin therapy. *Liver Int* 2011; **31**: 1359–65.
17 Enomoto N, Sakuma I, Asahina Y *et al.* Mutations in the nonstructural protein 5A gene and response to interferon in patients with chronic hepatitis C virus 1b infection. *N Engl J Med* 1996; **334**: 77–81.
18 Nakano I, Fukuda Y, Katano Y, Nakano S, Kumada T, Hayakawa T. Why is the interferon sensitivity-determining region (ISDR) system useful in Japan? *J Hepatol* 1999; **30**: 1014–22.
19 Pascu M, Martus P, Höhne M *et al.* Sustained virological response in hepatitis C virus type 1b infected patients is predicted by the number of mutations within the NS5A-ISDR: a meta-analysis focused on geographical differences. *Gut* 2004; **53**: 1345–51.
20 Yen YH, Hung CH, Hu TH *et al.* Mutations in the interferon sensitivity-determining region (nonstructural 5A amino acid 2209-2248) in patients with hepatitis C-1b infection and correlating response to combined therapy of pegylated interferon and ribavirin. *Aliment Pharmacol Ther* 2008; **27**: 72–9.
21 Muñoz de Rueda P, Casado J, Patón R *et al.* Mutations in E2-PePHD, NS5A-PKRBD, NS5A-ISDR, and NS5A-V3 of hepatitis C virus genotype 1 and their relationships to pegylated interferon-ribavirin treatment responses. *J Virol* 2008; **82**: 6644–53.
22 Gale M Jr, Blakely CM, Kwieciszewski B *et al.* Control of PKR protein kinase by hepatitis C virus nonstructural 5A protein: molecular mechanisms of kinase regulation. *Mol Cell Biol* 1998; **18**: 5208–18.
23 Sáiz JC, López-Labrador FX, Ampurdanés S *et al.* The prognostic relevance of the nonstructural 5A gene interferon sensitivity determining region is different in infections with genotype 1b and 3a isolates of hepatitis C virus. *J Infect Dis* 1998; **177**: 839–47.
24 Murakami T, Enomoto N, Kurosaki M, Izumi N, Marumo F, Sato C. Mutations in nonstructural protein 5A gene and response to interferon in hepatitis C virus genotype 2 infection. *Hepatology* 1999; **30**: 1045–53.
25 Sarrazin C, Kornetzky I, Rüster B *et al.* Mutations within the E2 and NS5A protein in patients infected with hepatitis C virus type 3a and correlation with treatment response. *Hepatology* 2000; **31**: 1360–70.
26 Dal Pero F, Tang KH, Gerotto M *et al.* Impact of NS5A sequences of Hepatitis C virus genotype 1a on early viral kinetics during treatment with peginterferon- alpha 2a plus ribavirin. *J Infect Dis* 2007; **196**: 998–1005.
27 Nagase Y, Yotsuyanagi H, Okuse C *et al.* Effect of treatment with interferon alpha-2b and ribavirin in patients infected with genotype 2 hepatitis C virus. *Hepatol Res* 2008; **38**: 252–8.
28 Hayashi K, Katano Y, Honda T *et al.* Mutations in the interferon sensitivity-determining region of hepatitis C virus genotype 2a correlate with response to pegylated-interferon-alpha 2a monotherapy. *J Med Virol* 2009; **81**: 459–66.
29 Ge D, Fellay J, Thompson AJ *et al.* Genetic variation in IL28B predicts hepatitis C treatment-induced viral clearance. *Nature* 2009; **461**: 399–401.
30 Otagiri H, Fukuda Y, Nakano I *et al.* Evaluation of a new assay for hepatitis C virus genotyping and viral load determination in patients with chronic hepatitis C. *J Virol Methods* 2002; **103**: 137–43.
31 Hayashi K, Fukuda Y, Nakano I *et al.* Prevalence and characterization of hepatitis C virus genotype 4 in Japanese hepatitis C carriers. *Hepatol Res* 2003; **25**: 409–14.
32 Simmonds P, Bukh J, Combet C *et al.* Consensus proposals for a unified system of nomenclature of hepatitis C virus genotypes. *Hepatology* 2005; **42**: 962–73.
33 Mangia A, Thompson AJ, Santoro R *et al.* An IL28B polymorphism determines treatment response of hepatitis C virus genotype 2 or 3 patients who do not achieve a rapid virologic response. *Gastroenterology* 2010; **139**: 821–7.

34 Akuta N, Suzuki F, Seko Y *et al.* Association of IL28B genotype and viral response of hepatitis C virus genotype 2 to interferon plus ribavirin combination therapy. *J Med Virol* 2012; **84**: 1593–9.
35 Akuta N, Suzuki F, Sezaki H *et al.* Association of amino acid substitution pattern in core protein of hepatitis C virus genotype 1b high viral load and non-virological response to interferon-ribavirin combination therapy. *Intervirology* 2005; **48**: 372–80.
36 Watanabe K, Yoshioka K, Yano M *et al.* Mutations in the nonstructural region 5B of hepatitis C virus genotype 1b: their relation to viral load, response to interferon, and the nonstructural region 5A. *J Med Virol* 2005; **75**: 504–12.
37 Katano Y, Hayashi K, Ishigami M *et al.* Association with 5′-untranslated region and response to interferon in chronic hepatitis C. *Hepatogastroenterology* 2007; **54**: 854–7.
38 El-Shamy A, Nagano-Fujii M, Sasase N *et al.* Sequence variation in hepatitis C virus nonstructural protein 5A predicts clinical outcome of pegylated interferon/ribavirin combination therapy. *Hepatology* 2008; **48**: 38–47.
39 Layden-Almer JE, Kuiken C, Ribeiro RM *et al.* Hepatitis C virus genotype 1a NS5A pretreatment sequence variation and viral kinetics in African American and white patients. *J Infect Dis* 2005; **192**: 1078–87.
40 Jenke AC, Moser S, Orth V, Zilbauer M, Gerner P, Wirth S. Mutation frequency of NS5A in patients vertically infected with HCV genotype 1 predicts sustained virological response to peginterferon alfa-2b and ribavirin combination therapy. *J Viral Hepat* 2009; **16**: 853–9.

J Gastroenterol (2013) 48:996–997
DOI 10.1007/s00535-012-0727-4

EDITORIAL

What is the benefit of computer-assisted image analysis of liver fibrosis area?

Kentaro Yoshioka

Received: 28 November 2012 / Accepted: 29 November 2012 / Published online: 15 December 2012

Liver fibrosis is usually semiquantitatively assessed in liver biopsy specimens by the numerical system of Scheuer [1], the Metavir group [2], or Ishak [3]. Fibrosis is staged as F0, no fibrosis; F1, portal fibrosis without septa; F2, portal fibrosis and few septa; F3, numerous septa without cirrhosis; and F4, cirrhosis. Staging mainly depends on the degree of the architectural changes of liver structure.

Computer-assisted image analysis of the stained fibrosis area in liver biopsy specimens is a method for quantitatively measuring the amount of liver fibrosis [4]. It is not used for the clinical assessment of liver fibrosis in general, but is often used in the assessment of fibrosis in animal models. Its low popularity in clinical practice may be attributed to the complexity of the method.

The fibrosis stage as determined by the numerical systems and the relative area of fibrosis measured by computer-assisted image analysis usually correlate well to each other. However, discrepancy between the two sometimes occurs. Which of the two is more useful in clinical practice may depend on the objectives of assessing liver fibrosis.

The current study by Isgro et al. showed that collagen proportionate area (CPA) has a better relationship with liver stiffness measurement (LSM) and with hepatic venous pressure gradient (HVPG) compared with the Ishak stage. They also reported that CPA at 1-year post-transplantation in hepatitis C virus-infected patients predicts subsequent clinical decompensation more accurately than Ishak stage or HVPG [5]. They conclude that CPA should be the histological parameter with which to compare LSM and other non-invasive fibrosis markers and also be used to subclassify cirrhosis.

Nitta et al. [6] also reported the good correlation between LSM and fibrosis area measured by image analysis in the patients with chronic hepatitis C, while LSM and Metavir score yielded better correlation. Xie et al. [7] reported that fibrosis area measured by image analysis significantly correlated with model for end-stage liver disease score, serum bilirubin levels and prothrombin time in the patients with hepatitis B virus-related decompensated cirrhosis.

Arima et al. [8] reported that 42 % of chronic hepatitis C patients with pretreatment F3-4 who obtained sustained virological response by interferon (IFN) therapy had decreased fibrosis assessed by the numerical staging system, while the fibrosis area measured by image analysis decreased in 92 %. Thus the computer-assisted image analysis of liver fibrosis is more sensitive to measure the reduction of liver fibrosis after IFN treatment than the numerical system.

In conclusion, the relative fibrosis area measured by computer-assisted image analysis is suitable for the comparison with newly developing non-invasive methods for fibrosis assessment, such as LSM. It is also useful to assess the degree of severe fibrosis in cirrhosis for predicting prognosis and to assess the change of fibrosis after antiviral treatment or in natural courses. It is better to add computer-assisted image analysis to the interpretation of liver biopsy in order to obtain valuable quantitative information in the specimens. The standardization and simplification of the method is needed in order that computer-assisted image analysis of fibrosis area will be widely used.

This comment refers to the article available at doi:10.1007/s00535-012-0694-9.

K. Yoshioka (✉)
Department of Liver, Biliary Tract and Pancreas Diseases, Fujita Health University, Toyoake, Aichi, Japan
e-mail: kyoshiok@fujita-hu.ac.jp

Conflict of interest K. Yoshioka received research grants from MSD K.K. and serves as a consultant to SANWA KAGAKU KENKYUSHO CO., LTD.

References

1. Scheuer PJ. Classification of chronic viral hepatitis: a need for reassessment. J Hepatol. 1991;13:372–4.
2. Intraobserver and interobserver variations in liver biopsy interpretation in patients with chronic hepatitis C. The French METAVIR Cooperative Study Group. Hepatology 1994;20:15–20.
3. Ishak K, Baptista A, Bianchi L, Callea F, De Groote J, Gudat F, et al. Histological grading and staging of chronic hepatitis. J Hepatol. 1995;22:696–9.
4. Goodman ZD, Becker RL Jr, Pockros PJ, Afdhal NH. Progression of fibrosis in advanced chronic hepatitis C: evaluation by morphometric image analysis. Hepatology. 2007;45:886–94.
5. Manousou P, Dhillon AP, Isgro G, Calvaruso V, Luong TV, Tsochatzis E, et al. Digital image analysis of liver collagen predicts clinical outcome of recurrent hepatitis C virus 1 year after liver transplantation. Liver Transpl. 2011;17:178–88.
6. Nitta Y, Kawabe N, Hashimoto S, Harata M, Komura N, Kobayashi K, et al. Liver stiffness measured by transient elastography correlates with fibrosis area in liver biopsy in patients with chronic hepatitis C. Hepatol Res. 2009;39:675–84.
7. Xie SB, Ma C, Lin CS, Zhang Y, Zhu JY, Ke WM. Collagen proportionate area of liver tissue determined by digital image analysis in patients with HBV-related decompensated cirrhosis. Hepatobiliary Pancreat Dis Int. 2011;10:497–501.
8. Arima M, Terao H, Kashima K, Arita T, Nasu M, Nishizono A. Regression of liver fibrosis in cases of chronic liver disease type C: quantitative evaluation by using computed image analysis. Intern Med. 2004;43:902–10.

Hepatology Research

Hepatology Research 2013; 43: 182–184 doi: 10.1111/j.1872-034X.2012.01096.x

Editorial

How to adjust the inflammation-induced overestimation of liver fibrosis using transient elastography?

See article in *Hepatology Research* 43: 185–191
Impact of mild to moderate elevations of alanine aminotransferase on liver stiffness measurement in chronic hepatitis B patients during antiviral therapy
Li-Bo Yan, Xia Zhu, Lang Bai, Ling-Bo Liang, En-Qiang Chen, Ling-Yao Du, Li-Chun Wang, Li-Yu Chen and Hong Tang

Transient elastography (TE) is a non-invasive reproducible method for measurement of liver stiffness (LSM). LSM correlates well with liver fibrosis stage. Thus, it has been hoped that TE will be able to replace liver biopsy which is problematic in its invasive nature, risk of complications and technical limitations derived from small sample sizes or interpretation variability. TE has been reported to provide useful clinical information based on the close correlation between LSM and liver fibrosis stage, such as appropriate time to start antiviral therapy, prediction of response to antiviral therapy, evaluation of effects of antiviral therapy, assessment of natural course of hepatitis and estimation of prognosis of hepatitis.[1]

However, LSM does not give us a completely corresponding estimation of fibrosis stage with liver biopsy. One of the reasons for this discrepancy is that LSM is affected by the histological findings other than liver fibrosis; such as edema, steatosis, inflammation or necrosis. Especially, inflammation has been reported to affect LSM in many reports. Acute or chronic inflammation can result in high LSM indicating the presence of falsely higher fibrosis stages than real fibrosis stages.[2–6] Thus, we have to establish a method to adjust the inflammation-induced overestimation of liver fibrosis using TE.

The current study by Yan *et al.* highlights some of the difficulties in adjusting the overestimation of fibrosis stage using TE in patients with liver inflammation. The authors studied the changes of LSM of the chronic hepatitis B patients with mild-to-moderate elevation of baseline alanine aminotransferase (ALT) levels (2–10-times the upper limit of normal [ULN]) treated with nucleoside/nucleotide analogs. This study shows that LSM decreased in parallel with the decline of ALT levels. The authors described that the decrease of LSM values is attributed mainly to amelioration of inflammation and maybe partially to regression of fibrosis. They report that pretreatment fibrosis stages of liver biopsies corresponded with LSM after normalization of ALT levels at a significantly higher rate than with baseline LSM in the patients of F0–1 (12/27 vs 23/25, $P < 0.001$), but not in those of F2–3 (4/12 vs 7/12, $P = 0.414$). They concluded that LSM became more accurate for the assessment of fibrosis stage after elevated ALT levels have been reduced to normal levels in chronic hepatitis B.

Although the approach of this study to adjust the inflammation-induced overestimation of fibrosis stage using TE is interesting and probably useful, its weakness is that the number of the patients studied is small; 25 patients of F0–1, 12 of F2–3 and four of F4. Additionally, in four of 12 patients of F2–3, fibrosis stages were underestimated by LSM both in pretreatment and after normalization of ALT levels. This finding indicates two facts. One is that we have to invent another method to adjust the overestimation of fibrosis stages for F2–3. The other is that there is also a problem of underestimation of liver fibrosis using TE. The mechanism of underestimation has not yet been elucidated. In addition, we need to know the correct fibrosis stages from LSM for determining how to treat the patients before treatment, but this study provides us the method to establish the fibrosis stage only after treatment.

It is important to determine the optimal time for restoring the reliability of LSM for assessing liver fibrosis after antiviral therapy or natural amelioration. Park *et al.* examined the decline of LSM and ALT levels in patients with chronic hepatitis B experiencing acute exacerbation.[7] Three months after acute exacerbation, ALT levels had decreased below two times the ULN and stabilized (medians, 522, 43, 21, 19, 18 and and 16 IU/L at baseline, 1, 3, 6, 9 and 12 months, respectively). However, LSM required 3 months more (6 months after exacer-

bation) for stabilization (median, 15.1, 10.0, 7.4, 7.1, 6.3 and 5.8 kPa at baseline, 1, 3, 6, 9 and 12 months, respectively). The authors conclude that LSM should be postponed for at least 3 months after stabilization of ALT levels below two times the ULN to restore the reliability of LSM in assessing liver fibrosis. Whether LSM at stabilization actually indicates the correct liver fibrosis stage should be also further studied.

Several reports suggested using different cut-off values for normal and elevated ALT levels in order to adjust the inflammation-induced overestimation of fibrosis stage using TE. As patients with higher ALT levels tend to have higher LSM than those with lower ALT levels at the same stage of liver fibrosis, the optimal cut-off values of LSM tend to be lower for the patients with normal ALT levels than those with elevated ALT levels. Chan *et al.* derived an algorithm using LSM to determine liver fibrosis in chronic hepatitis B.[8] An LSM of less than 5 kPa should indicate F0 regardless of ALT levels. For patients with normal ALT levels, an LSM of 5–6 kPa would indicate F0–2, an LSM of 6–9 kPa (gray zone) F0–4 (liver biopsy is recommended), an LSM of more than 9 kPa F3–4 and an LSM of more than 12 kPa F4. For patients with elevated ALT levels (>1–5-times ULN), an LSM of 5–7.5 kPa would indicate F0–2, an LSM of 7.5–12 kPa (gray zone) F0–4, an LSM of more than 12 kPa F3–4 and an LSM of more than 13.4 kPa F4. Chan *et al.* suggest that, based on these algorithms, liver biopsy can be avoided in 62% and 58% of normal and elevated ALT levels, respectively.

Kim *et al.* reported that the cut-off LSM values for F2 or higher, F3 or higher and F4 were 6.0, 7.5 and 10.1 kPa, respectively, in chronic hepatitis B patients with normal ALT levels, whereas they were 8.9, 11.0 and 15.5 kPa, respectively, in those with elevated ALT levels (>1–2-times ULN).[9]

Kim *et al.* also developed an LSM-based prediction model for cirrhosis using different cut-off values according to ALT levels in chronic hepatitis B.[10] They proposed LSM spleen diameter to platelet ratio index (LSPI): LSM × spleen diameter / platelet count × 100. In the whole cohort, LSPI cut-off values of 39 and 77 provided a negative predictive value (NPV) of 96.1% and positive predictive value (PPV) of 95.8%, respectively. 74.8% of the patients with LSPI of less than 39 or more than 77 could be diagnosed as non-cirrhotic or cirrhotic and avoid liver biopsy. In the patients with normal ALT levels, LSPI cut-off values of 38 and 62 provided an NPV of 95.7% and PPV of 95.5%, respectively. In those with elevated ALT levels, LSPI cut-off values of 42 and 94 provided an NPV of 95.1% and PPV of 96.4%, respectively. With this method, 76.7% of the patients can be diagnosed as non-cirrhotic or cirrhotic and avoid liver biopsy.

Acoustic radiation force impulse (ARFI) elastography can measure LSM and be used to assess the liver fibrosis stage as well as TE. Yoon *et al.* reported that the optimum cut-off values for ARFI elastography were 1.13 m/s for F2 or more and 1.98 m/s for F4; these decreased to 1.09 m/s for F2 or more and 1.81 m/s for F4 in patients with normal ALT levels.[11]

To adjust the inflammation-induced overestimation of liver fibrosis, two methods have been proposed. One is to wait until inflammation and its effect on LSM subside naturally or by antiviral treatment. This method has some problems; when is the optimal time for measurement of LSM and whether LSM at the point of normal ALT levels actually indicates real fibrosis stages. The other method is to use different cut-off values for the patients with normal ALT levels and those with elevated ALT levels. This method also has some problems. We should consider the degrees of ALT elevation. The cut-off values may have to differ according to the degrees of elevation of ALT levels. For example, the cut-off values should differ between the patients with ALT levels of 1–2-times ULN and those of 2–5-times ULN. There is also a question whether the degree of elevation of ALT levels actually correlate with elevation of LSM. Vigano *et al.* reported that LSM correlated significantly with bilirubin only and that the decline of LSM significantly correlated with bilirubin in acute hepatitis B.[12] In addition, the degrees of inflammation-induced overestimation differ among the different fibrosis stages. Nitta *et al.* reported that LSM significantly correlated with ALT levels only in F2, but not in the other fibrosis stages.[5] Arena *et al.* also reported that the presence of inflammation significantly affected LSM in patients who did not have cirrhosis.[6]

In conclusion, TE is a non-invasive and reproducible method for measuring LSM and assessing liver fibrosis stages, which may hopefully replace liver biopsy. Inflammation can result in high LSM values indicating the presence of falsely higher fibrosis stages than real fibrosis stages. Several studies have recommended methods to adjust the inflammation-induced overestimation of liver fibrosis using TE, but the results are not yet satisfactory to use them in clinical practice. Thus, further studies are needed.

Kentaro Yoshioka
Department of Liver, Biliary Tract and Pancreas Diseases, Fujita Health University, Toyoake, Japan

REFERENCES

1 Yoshioka K, Hashimoto S. Can non-invasive assessment of liver fibrosis replace liver biopsy? *Hepatol Res* 2012; **42**: 233–40.
2 Coco B, Oliveri F, Maina AM *et al.* Transient elastography: a new surrogate marker of liver fibrosis influenced by major changes of transaminases. *J Viral Hepat* 2007; **14**: 360–9.
3 Oliveri F, Coco B, Ciccorossi P *et al.* Liver stiffness in the hepatitis B virus carrier: a non-invasive marker of liver disease influenced by the pattern of transaminases. *World J Gastroenterol* 2008; **14**: 6154–62.
4 Tapper EB, Cohen EB, Patel K *et al.* Levels of alanine aminotransferase confound use of transient elastography to diagnose fibrosis in patients with chronic hepatitis C virus infection. *Clin Gastroenterol Hepatol* 2012; **10**: 932–7.
5 Nitta Y, Kawabe N, Hashimoto S *et al.* Liver stiffness measured by transient elastography correlates with fibrosis area in liver biopsy in patients with chronic hepatitis C. *Hepatol Res* 2009; **39**: 675–84.
6 Arena U, Vizzutti F, Abraldes JG *et al.* Reliability of transient elastography for the diagnosis of advanced fibrosis in chronic hepatitis C. *Gut* 2008; **57**: 1288–93.
7 Park H, Kim SU, Kim D *et al.* Optimal time for restoring the reliability of liver stiffness measurement in patients with chronic hepatitis B experiencing acute exacerbation. *J Clin Gastroenterol* 2012; **46**: 602–7.
8 Chan HL, Wong GL, Choi PC *et al.* Alanine aminotransferase-based algorithms of liver stiffness measurement by transient elastography (Fibroscan) for liver fibrosis in chronic hepatitis B. *J Viral Hepat* 2009; **16**: 36–44.
9 Kim SU, Kim Y, Park JY *et al.* How can we enhance the performance of liver stiffness measurement using FibroScan in diagnosing liver cirrhosis in patients with chronic hepatitis B? *J Clin Gastroenterol* 2010; **44**: 66–71.
10 Kim BK, Han KH, Park JY *et al.* A novel liver stiffness measurement-based prediction model for cirrhosis in hepatitis B patients. *Liver Int* 2010; **30**: 1073–81.
11 Yoon KT, Lim SM, Park JY *et al.* Liver stiffness measurement using acoustic radiation force impulse (ARFI) elastography and effect of necroinflammation. *Dig Dis Sci* 2012; **57**: 1682–91.
12 Vigano M, Massironi S, Lampertico P *et al.* Transient elastography assessment of the liver stiffness dynamics during acute hepatitis B. *Eur J Gastroenterol Hepatol* 2010; **22**: 180–4.

World Journal of Gastroenterology

Online Submissions: http://www.wjgnet.com/esps/
wjg@wjgnet.com
doi:10.3748/wjg.v19.i20.3165

World J Gastroenterol 2013 May 28; 19(20): 3165-3168
ISSN 1007-9327 (print) ISSN 2219-2840 (online)

CASE REPORT

Behçet's disease complicated by multiple aseptic abscesses of the liver and spleen

Keisuke Maeshima, Koji Ishii, Megumi Inoue, Katsuro Himeno, Masataka Seike

Keisuke Maeshima, Koji Ishii, Megumi Inoue, Katsuro Himeno, Masataka Seike, Department of Internal Medicine I, Faculty of Medicine, Oita University, Oita 879-5593, Japan
Author contributions: Maeshima K and Inoue M co-wroted the paper; Ishii K, Himeno K and Seike M performed the treatment of the patient; all authors discussed and commented on the manuscript.
Correspondence to: Koji Ishii, MD, PhD, Department of Internal Medicine I, Faculty of Medicine, Oita University, 1-1 Idaigaoka, Hasama-machi, Yufu, Oita 879-5593, Japan. kois@oita-u.ac.jp
Telephone: +81-97-5865793 Fax: +81-97-5494480
Received: October 18, 2012 Revised: March 1, 2013
Accepted: March 8, 2013
Published online: May 28, 2013

Abstract

Aseptic abscesses are an emergent entity and have been described in inflammatory bowel disease, especially in Crohn's disease, and in other diseases. However, aseptic abscesses associated with Behçet's disease are extremely rare. We report a Japanese male diagnosed with an incomplete type of Behçet's disease who developed multiple aseptic abscesses of the spleen and liver. In 2002, the spleen abscesses were accompanied by paroxysmal oral aphthous ulcers and erythema nodosum. As the patient's response to antibiotic treatment was inadequate, a splenectomy was performed. Severe inflammatory cell infiltration, largely of polymorphonuclear neutrophils, was observed without evidence of bacterial or fungal growth. Although the patient had no history of ocular symptoms or genital ulcers, a diagnosis of incomplete Behçet's disease was made according to the Japanese diagnostic criteria because of the presence of paroxysmal arthritis and epididymitis since 2002. In 2005, multiple liver abscesses developed with right hypochondrial pain and seemed to be attributed to Behçet's disease because the abscesses yielded negative results during a microbiologic investigation and failed to go into remission under antibiotic therapy. Oral prednisone (15 mg/d) was started in May 2006, and the abscesses dramatically disappeared 4 wk after treatment. Although the patient had a relapse of the liver abscesses in association with the tapering of prednisone, the augmentation of prednisone dosage yielded a response. The abscesses of the liver and spleen were strongly suggested to be attributed to Behçet's disease. Clinician should be aware of the existence of aseptic abscesses as uncommon manifestations of Behçet's disease.

Key words: Behçet's disease; Aseptic abscess; Spleen; Liver; Prednisone

Core tip: We report a Japanese male diagnosed with an incomplete type of Behçet's disease who developed multiple aseptic abscesses of the spleen and liver. Spleen abscesses developed with paroxysmal oral aphthous ulcers and erythema nodosum. A splenectomy was performed, and severe neutrophil infiltration was observed without evidence of bacterial or fungal growth. Multiple liver abscesses also developed with right hypochondrial pain and seemed to be attributed to Behçet's disease because the abscesses yielded negative results during a microbiologic investigation. Oral prednisone (15 mg/d) was started, and the abscesses dramatically disappeared. Clinicians should be aware of the existence of aseptic abscesses as uncommon manifestations of Behçet's disease.

Maeshima K, Ishii K, Inoue M, Himeno K, Seike M. Behçet's disease complicated by multiple aseptic abscesses of the liver and spleen. *World J Gastroenterol* 2013; 19(20): 3165-3168 Available from: URL: http://www.wjgnet.com/1007-9327/full/v19/i20/3165.htm DOI: http://dx.doi.org/10.3748/wjg.v19.i20.3165

INTRODUCTION

Behçet's disease (BD) is a systemic inflammatory disease commonly characterized by oral and genital ulcerations, with involvement of the skin and eye. The manifestations of BD are protean, and all symptoms and signs tend to recur either alone or in combination. Aseptic abscesses (AAs) are characterized by deep, sterile, round lesions consisting of neutrophil infiltration that do not respond to antibiotic therapy but improve with corticosteroid and immunosuppressive drugs. Clinical reports and case series concerning AAs in patients with inflammatory bowel disease, neutrophilic dermatoses, and other diseases have been published[1-5]. Although BD belongs to a group of neutrophilic dermatoses, AAs associated with BD are extremely rare. Here, we describe a patient with BD complicated by AAs of the liver and spleen, which were successfully treated with corticosteroid therapy.

CASE REPORT

In February 2006, a 20-year-old Japanese male suffering from multiple liver abscesses associated with sporadic fever, right hypochondrial pain, and elevated inflammatory markers was admitted to our hospital. In 2002, at the age of 16, he developed oral aphthous ulcers, erythema nodosum, pericardial effusion, and multiple spleen abscesses (Figure 1A). As for the aphthous ulcers and erythema nodosum, resolution occurred spontaneously. Pericardiocentesis was performed. Effusive pericarditis was thought to be the cause of the pericardial fluid; however, it did not reaccumulate after pericardiocentesis. Because empirical antibiotic therapy had the least effect and symptoms such as fever and left hypochondrial pain persisted, an open splenectomy was performed in October 2002. Upon macroscopic examination, sections of the resected spleen showed multiple yellow nodular lesions (10-20 mm in diameter) (Figure 1B). Pathological examination confirmed the presence of severe inflammatory cell infiltration, largely of polymorphonuclear neutrophils, without evidence of bacterial or fungal growth. In addition to oral aphthosis and erythema nodosum, the primary symptoms of BD, paroxysmal arthritis and epididymitis have occurred since 2002. Although the patient had no history of ocular symptoms or genital ulcers, a diagnosis of incomplete BD was made according to the criteria of the BD Research Committee of Japan[6]. Spleen abscesses were suspected to be attributed to BD, but the association was difficult to prove. Paroxysmal oral aphthosis and arthritis persisted after splenectomy, and at the age of 19 in March 2005, multiple abscesses with an aggressive inflammatory response developed in the liver. Antibiotics were unable to demonstrate any benefit, and the liver abscesses seemed to be attributed to BD. Colchicine (with a 1.5 mg maximum daily dose) was started in July 2005. However, the patient had elevated inflammatory markers, fever, and right hypochondrial pain.

Upon physical examination, the patient did not present with fever, oral aphthosis, erythema nodosum, articular swelling, or abdominal tenderness at the time. The

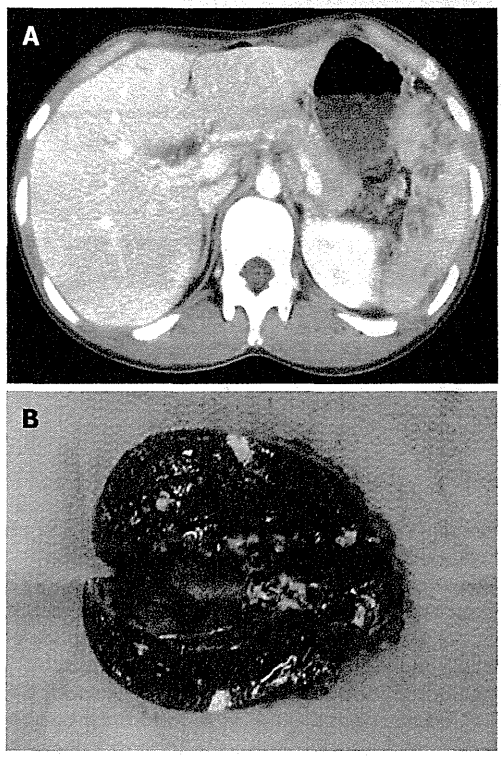

Figure 1 Contrast-enhanced abdominal computed tomography scan showing multiple spleen abscesses (A), and macroscopic findings of the cut surface of the resected spleen (B).

findings from the laboratory examinations are summarized as follows: white blood cell count, 13400/L (normal: 4000-9000/L) with 69% neutrophils; hemoglobin, 14.8 g/dL (normal: 12.0-16.0 g/dL); platelets, 57.1 $\times$ 10^4/L (normal: 14.0-40.0 $\times$ 10^4/L); aspartate aminotransferase, 21 U/L (normal: 10-40 U/L); alanine aminotransferase, 30 U/L (normal: 5-40 U/L); lactate dehydrogenase, 137 U/L (normal: 115-245 U/L); total bilirubin, 0.4 mg/dL (normal: 0.3-1.2 mg/dL); alkaline phosphatase, 583 U/L (normal: 115-359 U/L); gamma-glutamyl transferase, 123 U/L (normal: $\leqslant$ 70 U/L); and C-reactive protein (CRP), 11.0 mg/dL (normal: $<$ 0.3 mg/dL). The results of the kidney function tests were within the normal limits. Antinuclear antibodies (speckled staining pattern) showed a 40-fold positive result (normal: $<$ 40-fold). Rheumatoid factor, antineutrophil cytoplasmic antibodies, and HLA-B51 antigen were negative (HLA-A24, B52, and B60 antigens were positive). Colonoscopy showed only a small aphthous ulcer in the terminal ileum; pathological examination showed non-specific chronic inflammation without any evidence of Crohn's disease (CD), such as noncaseating granuloma. Blood and urine cultures were negative. An abdominal ultrasound scan was performed, which showed multiple round lesions in the liver. Contrast-enhanced abdominal computed tomography scan demonstrated multiple areas of low-attenuation with ring enhancement in the liver (Figure 2A). Despite empirical antibiotic therapy, no clinical improvement was achieved. Ultrasound-guided percutaneous aspiration of the abscess yielded pus containing numerous neutrophils; no

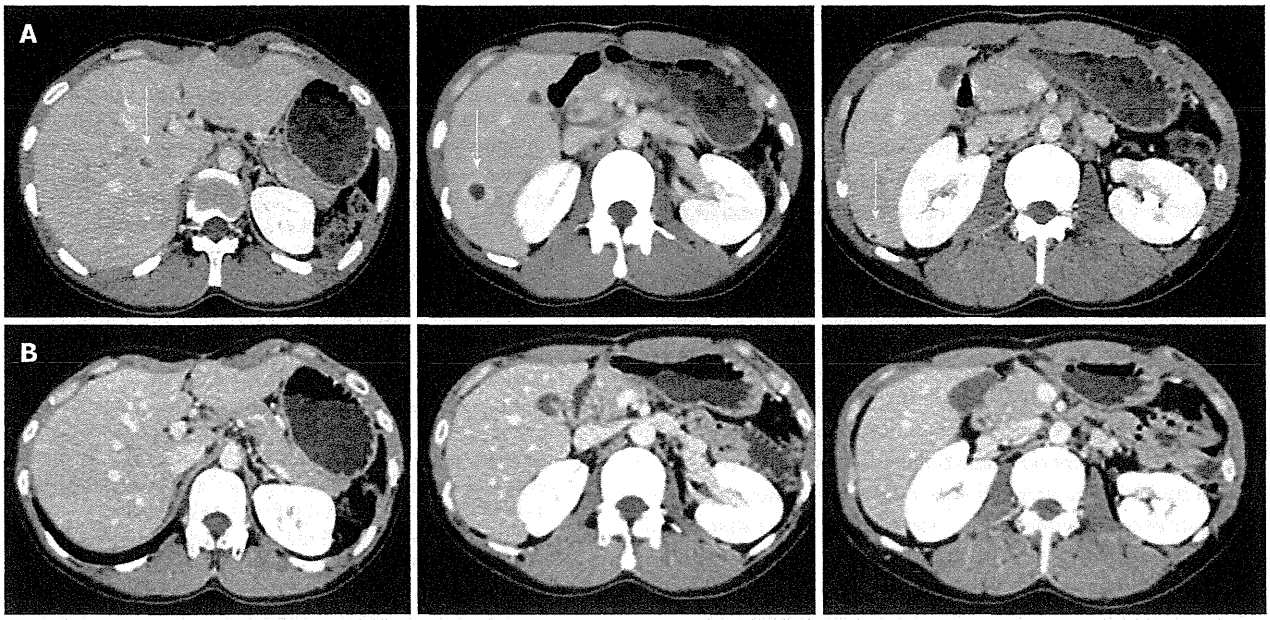

Figure 2 Contrast-enhanced abdominal computed tomography scan showing multiple liver abscesses (arrow) before (A) and 4 wk after corticosteroid therapy (B). Multiple areas of low-attenuation with ring enhancement were seen in the liver as indicated by the arrows (A). However, the areas vanished after treatment (B).

microbes were found in the culture. A fine needle biopsy of the liver lesions was performed, and a pathological examination revealed necrotic tissue containing inflammatory cells. Based on this evidence, these lesions were interpreted as aseptic liver abscesses associated with BD, and oral low-dose prednisone (15 mg/d), in addition to colchicine, was initiated in May 2006. A rapid improvement in the patient's symptoms occurred; the levels of CRP and liver enzymes reached normal range, and the liver abscesses disappeared within 4 wk of the initiation of corticosteroid therapy (Figure 2B). The dose of prednisone was gradually tapered; at 7.5 mg/d prednisone, however, the CRP level increased again, requiring a higher dose of prednisone. Therefore, the patient was maintained on low-dose prednisone therapy (10-12.5 mg/d) to restrain the inflammatory response. Elevated CRP was observed without obvious abnormality in August 2010, and the recurrence of AAs in the liver was detected by abdominal CT without abdominal symptoms in August 2011. After escalating the dose of prednisone to 20 mg/d, the liver abscesses vanished once again. The dose of prednisone was gradually tapered to 15 mg/d, and complete clearance of the liver lesions was achieved in February 2012.

DISCUSSION

We present a patient with BD who developed AAs in the spleen and liver. AAs are an emergent entity. This condition has been described in inflammatory bowel disease (IBD), especially in CD, as well as in other diseases such as Sweet's syndrome and pyoderma gangrenosum[1-5]. Most patients with AAs have some underlying disease, and it has been proposed that AAs belong to the spectrum of autoinflammatory multifactorial disorders[1]. The diagnosis of AAs is of exclusion on the basis of the following criteria suggested by André *et al*[1]: (1) deep abscess(es) upon radiologic examination, with neutrophilic features proven by surgical pathology or aspiration when performed; (2) negative blood cultures, negative serologic tests for bacteria, and, when surgical procedure or aspiration are performed, sterile standard, acid-fast bacillus and fungal cultures of pus; (3) failure of antibiotic therapy; and (4) rapid improvement by corticosteroids, sometimes in combination with immunosuppressive drugs. The main clinical manifestations of AAs are fever, abdominal pain, and weight loss. A rare case of BD complicated by multiple intrahepatic abscesses, which was dramatically resolved by antibiotic therapy, was reported[7]. There is also a case report of BD that was suspected to be complicated by sterile cerebral abscesses, although the clinical state of the patient gradually improved without immunosuppressive therapy[8]. In our patient, the liver and spleen abscesses were negative upon microbiologic investigation, and remission was not achieved under antibiotic therapy. Furthermore, the rapid resolution of the abscesses with corticosteroid therapy, even at the time of disease relapse in association with the tapering of prednisone, also favored a diagnosis of BD-associated AAs. Based on a PubMed search of the literature, our patient is the first unfailing case of sterile visceral abscesses associated with BD.

A differential diagnosis of CD *vs* BD can be difficult. Although ulcerative lesions at the ileocecal area are common in both diseases, we diagnosed the patient as having intestinal BD because of a lack of factors suggestive of CD: there was only one ulcerative lesion, its shape was not longitudinal, and histopathological examination showed no granulomatous lesions. It is also often difficult to dif-

ferentiate incomplete types of BD from Sweet's syndrome because some overlapping manifestations exist between BD and Sweet's disease. Unfortunately, a skin biopsy was not performed. However, we are convinced of the diagnosis of incomplete BD in this case because our patient had a chronic course with remissions and relapses, as well as a history of epididymitis and pericarditis, found in relatively rare manifestations of BD[9].

Neutrophilic dermatoses are well-recognized cutaneous manifestations of systemic diseases such as IBD, and the wide spectrum of the disease includes Sweet's syndrome and pyoderma gangrenosum. These diseases may share common features such as sterile infiltration of polymorphonuclear leukocytes; BD is analogous to this condition[10]. Extracutaneous neutrophilic infiltrates are observed in all forms of neutrophilic dermatoses, but they predominate in Sweet's syndrome[11]. Sweet's syndrome associated with BD has been reported, and there may be similarities in the pathogenesis of BD and Sweet's disease[12]. Therefore, it seems reasonable that BD was complicated by AAs, although the mechanism remains unclear. Classically, Th1 immune response polarization has been known to be the main characteristic of BD immunopathogenesis[13]. The interleukin 17 (IL-17)-mediated (Th17) immune response may also contribute to immunological aberrations of BD[14]. IL-8-producing T cells were suggested to orchestrate neutrophil-rich pathologies of BD[15]. It was proposed that liver disease occurring in IBD is mediated by an aberrant homing of gut-derived T cells to the liver, with subsequent extensive lymphocyte infiltration of the liver[16]. Therefore, the mechanism by which AAs of the liver and spleen occurred in our case might be explained by an aberrant T cell-mediated immune response.

A patient with CD and associated AAs who underwent successful splenectomy was reported[17]. However, in our study, the patient developed AAs in the liver after splenectomy and finally needed immunosuppressive therapy. The risks of postoperative infection and thrombosis after splenectomy are now widely accepted. Accordingly, splenectomy as a treatment option might not be advisable in cases of AAs associated with BD.

In conclusion, we present a case of aseptic liver and spleen abscesses as the presenting picture of incomplete BD, in which complete remission was only obtained by corticosteroid therapy. The current case illustrates the possibility of the existence of AAs as uncommon manifestations of BD. Thus, physicians should be aware of this possibility to avoid a delay in diagnosis and unnecessarily aggressive therapies such as splenectomy.

REFERENCES

1 **André MF**, Piette JC, Kémény JL, Ninet J, Jego P, Delèvaux I, Wechsler B, Weiller PJ, Francès C, Blétry O, Wismans PJ, Rousset H, Colombel JF, Aumaître O. Aseptic abscesses: a study of 30 patients with or without inflammatory bowel disease and review of the literature. *Medicine (Baltimore)* 2007; **86**: 145-161 [PMID: 17505254 DOI: 10.1097/md.0b013e18064f9f3]

2 **Quilichini R**, Mazzerbo F, Baume D, Carsuzaa F, Burtey S. [Sweet's syndrome and aseptic abscess of the spleen]. *Rev Med Interne* 1996; **17**: 1029-1031 [PMID: 9008752]

3 **Klinger S**, Mathis N, Jackson S. Bullous Sweet syndrome associated with an aseptic splenic abscess. *Cutis* 2009; **84**: 255-258 [PMID: 20099618]

4 **Fukuhara K**, Urano Y, Kimura S, Hori K, Arase S. Pyoderma gangrenosum with rheumatoid arthritis and pulmonary aseptic abscess responding to treatment with dapsone. *Br J Dermatol* 1998; **139**: 556-558 [PMID: 9767321]

5 **Zakout R**, Fonseca M, Santos JM, Marques A, Távora I, Oliveira E, Ferreira C, Victorino RM. Multiple aseptic liver abscesses as the initial manifestation of Crohn's disease: report of a case. *Dis Colon Rectum* 2009; **52**: 343-345 [PMID: 19279433 DOI: 10.1007/DCR.0b013e318199db60]

6 **Suzuki Kurokawa M**, Suzuki N. Behcet's disease. *Clin Exp Med* 2004; **4**: 10-20 [PMID: 15598081]

7 **Gelber AC**, Schachna L, Mitchell L, Schwartzman G, Hartnell G, Geschwind JF. Behçet's disease complicated by pylephlebitis and hepatic abscesses. *Clin Exp Rheumatol* 2001; **19**: S59-S61 [PMID: 11760402]

8 **Tokgoz S**, Ogmegul A, Mutluer M, Kivrak AS, Ustun ME. Cerebral abscesses in Behcet's disease: a case report. *Turk Neurosurg* 2012; **22**: 116-118 [PMID: 22274984 DOI: 10.5137/1019-5149.JTN.3297-10.2]

9 **Sezen Y**, Buyukhatipoglu H, Kucukdurmaz Z, Geyik R. Cardiovascular involvement in Behçet's disease. *Clin Rheumatol* 2010; **29**: 7-12 [PMID: 19830382 DOI: 10.1007/s10067-009-1302-0]

10 **Yim CW**, White RH. Behçet's syndrome in a family with inflammatory bowel disease. *Arch Intern Med* 1985; **145**: 1047-1050 [PMID: 4004429]

11 **Vignon-Pennamen MD**. The extracutaneous involvement in the neutrophilic dermatoses. *Clin Dermatol* 2000; **18**: 339-347 [PMID: 10856666]

12 **Wu F**, Luo X, Yuan G. Sweet's syndrome representing a flare of Behçet's disease. *Clin Exp Rheumatol* 2009; **27**: S88-S90 [PMID: 19796541]

13 **Frassanito MA**, Dammacco R, Cafforio P, Dammacco F. Th1 polarization of the immune response in Behçet's disease: a putative pathogenetic role of interleukin-12. *Arthritis Rheum* 1999; **42**: 1967-1974 [PMID: 10513814]

14 **Leng RX**, Chen GM, Pan HF, Ye DQ. The role of IL-23/IL-17 axis in the etiopathogenesis of Behçet's disease. *Clin Rheumatol* 2010; **29**: 1209 [PMID: 20625913 DOI: 10.1007/s10067-010-1531-2]

15 **Keller M**, Spanou Z, Schaerli P, Britschgi M, Yawalkar N, Seitz M, Villiger PM, Pichler WJ. T cell-regulated neutrophilic inflammation in autoinflammatory diseases. *J Immunol* 2005; **175**: 7678-7686 [PMID: 16301678]

16 **Adams DH**, Eksteen B. Aberrant homing of mucosal T cells and extra-intestinal manifestations of inflammatory bowel disease. *Nat Rev Immunol* 2006; **6**: 244-251 [PMID: 16498453 DOI: 10.1038/nri1784]

17 **Renna S**, Mocciaro F, Perricone G, Orlando A, Virdone R, Speciale A, Lima G, Stella M, Cottone M. Is splenectomy a treatment option for aseptic abscesses in patients with Crohn's disease? *Eur J Gastroenterol Hepatol* 2009; **21**: 1314-1316 [PMID: 19474741 DOI: 10.1097/MEG.0b013e32832bab85]

P- Reviewers Andre MFJ, Zippi M **S- Editor** Song XX
L- Editor A **E- Editor** Zhang DN

Nephrol Dial Transplant (2013) 28: 1120–1130
doi: 10.1093/ndt/gfs440
Advance Access publication 9 December 2012

ndt
Nephrology Dialysis Transplantation

Original Articles

Obesity-related chronic kidney disease is associated with spleen-derived IL-10

Koro Gotoh,
Megumi Inoue,
Takayuki Masaki,
Seiichi Chiba,
Kentaro Shiraishi,
Takanobu Shimasaki,
Kazue Matsuoka,
Hisae Ando,
Kansuke Fujiwara,
Naoya Fukunaga,
Kohei Aoki,
Tomoko Nawata,
Isao Katsuragi,
Tetsuya Kakuma,
Masataka Seike
and Hironobu Yoshimatsu

Department of Internal Medicine 1, Faculty of Medicine, Oita University, Hasama, Yufu, Japan

Correspondence and offprint requests to: Koro Gotoh; E-mail: gotokoro@oita-u.ac.jp

Keywords: chronic kidney disease, IL-10, inflammation, obesity, spleen

ABSTRACT

Background. Obesity is associated with systemic low-grade inflammation and is a risk factor for chronic kidney disease (CKD), but the molecular mechanism remains uncertain. We noticed spleen-derived interleukin (IL)-10 because it is observed that obesity reduces several cytokines in the spleen.

Methods. We examined whether spleen-derived IL-10 regulates CKD caused by a high-fat diet (HF)-induced obesity as follows: (i) male mice were fed with HF (60% fat) during 8 weeks and IL-10 induction from the spleen was examined, (ii) glomerular hypertrophy, fibrosis, inflammatory responses in the kidney and systolic blood pressure (SBP) were evaluated in splenectomy (SPX)-treated mice fed HF, (iii) exogenous IL-10 was systemically administered to HF-induced obese mice and the alteration of obesity-induced pathogenesis caused by IL-10 treatment was assessed. (iv) IL-10 knockout (IL-10KO) mice were treated with SPX and glomerular hypertrophy, fibrosis and the inflammatory condition in the kidney and SBP were also investigated.

Results. Obesity decreased serum levels of only IL-10, an anti-inflammatory cytokine even though pro- and anti-inflammatory cytokine expression in the spleen was significantly lower in the obese group. SPX aggravated HF-induced inflammatory responses in the kidney and hypertension. These HF-induced alterations were inhibited by systemically administered IL-10. Moreover, SPX had little effect on inflammatory responses and SBP in the kidney of IL-10KO mice.

Conclusions. We suggest that obesity reduces IL-10 induction from the spleen, and spleen-derived IL-10 may protect against the development of CKD induced by obesity.

INTRODUCTION

Obesity leads to the infiltration of fat in multiple organs, including the liver, heart and kidneys. Obese conditions increase fatty acid flux to the liver and pancreas [1, 2]. Infiltration of the liver by fat, or nonalcoholic fatty liver disease (NAFLD), is a major form of chronic liver disease in adults and children [3]. Recent studies have reported that high-fat diet (HF)-fed mice show several types of renal damage, and obesity is believed to have a direct role in the pathogenesis of chronic kidney disease (CKD). Pathological studies have demonstrated that subjects with severe obesity develop proteinuria with pathological findings of podocyte hypertrophy, mesangial expansion, glomerular enlargement, and focal segmental diabetes and hypertension [4, 5]. Obesity is a common risk factor for CKD and NAFLD, and it is not surprising that the two conditions are associated [6, 7].

The spleen is the largest lymphoid organ in the body and plays an important role in the host immune function. Obese rats show decreased expression of pro-inflammatory cytokines such as interleukin (IL)-6 and tumor necrosis factor-α (TNF-α) in the spleen [8]. In contrast, IL-10 is a potent anti-inflammatory cytokine that inhibits the synthesis of pro-inflammatory cytokines. It is synthesized by several cell types within multiple organs, including the spleen. Large amounts of IL-10 are produced by activated B cells, which mature in the marginal zone of the spleen. New evidence has shown that IL-10-producing B cells play a regulatory role in suppressing harmful immune responses [9]. In fact, low IL-10 production capacity has been demonstrated in obesity [10, 11]. Based on these findings, obesity is hypothesized to suppress IL-10 synthesis, resulting in chronic kidney inflammation. Our data demonstrate that obesity reduced IL-10 expression in the spleen and that spleen-derived IL-10 protected against inflammatory responses induced by obesity in the kidney.

MATERIALS AND METHODS

Animals

Male C57Bl/6J mice (wild-type mice, 22–25 g; KBT Oriental, Japan) and IL-10-deficient mice (IL-10KO mice, 002251-B6.129P2-*Il10*^{tm1Cgn}/J, a gift from Sandy Morse, The Jackson Laboratory, Bar Harbor, ME, USA) were housed in a room at Oita University under a 12/12-h light/dark cycle with lights on from 07:00 to 19:00. IL-10KO mice maintained at our university were used for backcrossing. Polymerase chain reaction primers of 5′-CCACACGCGTCACCTTAATA-3′ (mutant forward), 5′-GTTATTGTCTTCCCGGCTGT-3′ (wild-type reverse) and 5′-CTTGCACTACCAAAGCCACA-3′ (common) were used for genotyping. All studies were conducted in accordance with Oita University guidelines, based on the Guide for the Care and Use of Laboratory Animals published by the US National Institutes of Health.

Experimental protocol

Experiment 1. Wild-type mice were assigned to one of two groups ($n = 6$ in each group) as follows: Group 1, mice were fed standard chow (standard: 20% fat, 56% carbohydrate, 24% protein; Diet Research, New Brunswick, NJ, USA) for 8 weeks and then subjected to sham operation (Sham); Group 2, mice were fed standard chow for 8 weeks and then underwent splenectomy (SPX). Anesthesia was then induced by intraperitoneal injection of sodium pentobarbital (50 mg/kg), the abdominal cavity was opened and the spleen was carefully removed. The abdomen was opened, but the spleen was not removed in the sham group.

Experiment 2. Wild-type mice were assigned to one of four groups ($n = 6$ in each group) as follows: Group 1, mice were fed standard chow for 8 weeks after sham operation and administered mouse serum albumin (m-albumin); Group 2, mice were fed a HF (60% fat, 20% carbohydrate, 20% protein; Diet Research) for 8 weeks after sham operation and then given m-albumin; Group 3, mice were fed HF for 8 weeks after SPX and then given m-albumin; Group 4, mice were fed HF for 8 weeks after sham operation and then given recombinant mouse IL-10 (r-IL-10, 0.5 ng/day; Wako Chemicals, Osaka, Japan).

Experiment 3. Wild-type and IL-10KO mice were assigned to one of three groups ($n = 6$ per each group) as follows: Group 1, mice were fed HF for 8 weeks after sham operation and administered m-albumin; Group 2, mice were fed HF for 8 weeks after SPX and administered m-albumin; Group 3, mice were fed HF for 8 weeks after SPX and administered r-IL-10 (0.5 ng/day; Wako Chemicals). Body weight was measured between 17:00 and 18:00 h. All mice were housed for an additional 4 weeks after completion of the interventions.

Cytokine levels in the spleen, kidney and serum

Commercial enzyme-linked immunosorbent assay (ELISA) kits (Invitrogen, Carlsbad, CA, USA) were used to measure the TNF-α, IL-1β, monocyte chemotactic protein-1 (MCP-1), IL-10, IL-4 and IL-13 levels in the spleen, kidney and serum. Neutrophil gelatinase-associated lipocalin (NGAL), an early biomarker of acute kidney injury, levels in the kidney were also measured using the NGAL ELISA kit (BioPorto, Gentofte, Denmark). Protein concentrations in each organ were analyzed using the Lowry method.

Table 1. Effects of HF feeding on splenic and serum levels of pro- and anti-inflammatory cytokines

	TNF-α	IL-1β	MCP-1	IL-4	IL-10	IL-13
Spleen (pg/mg protein)						
Standard	85.2 ± 6.5	42.8 ± 5.1	16.9 ± 1.7	24.5 ± 3.7	20.2 ± 2.5	9.7 ± 1.2
HF	52.8 ± 7.3*	25.7 ± 3.1*	9.0 ± 1.4*	16.7 ± 3.5*	9.3 ± 1.1*	7.1 ± 1.4*
Serum (pg/mL)						
Standard	24.1 ± 8.2	12.9 ± 5.8	19.1 ± 4.1	31.1 ± 7.3	30.5 ± 4.8	5.6 ± 1.2
HF	29.7 ± 6.8	17.7 ± 3.9	21.1 ± 3.4	28.0 ± 7.2	18.2 ± 3.7*	4.9 ± 1.4

Protein levels of TNF-α, IL-1β, MCP-1, IL-4, IL-10 and IL-13 in spleens and serum from each group ($n = 6$).
*$P < 0.05$ versus the standard group. Treatment groups: standard, fed a standard chow and given a sham operation. HF, fed a HF and given a sham operation.

Western blotting

Frozen tissue preparations were homogenized with sample buffer, centrifuged and boiled. Total protein concentration of tissues was quantified using the Bradford method. Equal amounts of total protein were loaded on 8% sodium dodecyl sulfate-polyacrylamide gels for electrophoresis and then electrophoretically transferred to polyvinylidene difluoride membranes (Bio-Rad, Hercules, CA, USA). The membranes were blocked with 5% nonfat milk for 1 h, incubated overnight with primary antibodies at 4°C and then incubated with a secondary antibody for 1 h at room temperature. The primary antibody solutions consisted of polyclonal antisera with specificity for rabbit desmin and nephrin (Acris Antibodies, Inc., San Diego, CA, USA). Desmin and nephrin were detected by enhanced chemiluminescence (Amersham Life Sciences, Fairfield, CT, USA) and quantified using Quantity One® imaging software (Bio-Rad).

Histological and immunohistochemical analyses

Kidney samples were fixed in 4% buffered paraformaldehyde, embedded in paraffin, sectioned and deparaffinized in xylene. Samples were examined with periodic acid-Schiff (PAS) and Mallory-Azan reagents.

For immunohistochemical staining of F4/80 and NGAL, 5-μm-thick frozen kidney sections were incubated overnight at 4°C with rabbit anti-mouse F4/80 (Acris Antibodies GmbH, Herford, Germany). Slides were subsequently washed with phosphate-buffered saline and incubated with biotin-conjugated goat anti-rabbit IgG (ABC reagent; Vector Laboratories, Burlingame, CA, USA). The immunoreactivity of each sample was visualized with diaminobenzidine (Nacalai Tesque, Kyoto, Japan). Immunostaining sections were counterstained with hematoxylin to identify the cell nuclei. The F4/80-positive cells were counted in 10 randomly chosen field (×400) within the same section of the renal cortex from an individual mouse. Staining was quantified using a 0.02-mm^2 graticulate eyepiece and expressed as cells per mm^2. Counting of individual glomeruli and tubulointerstitial areas within 10 selected fields included more than 50 glomeruli and 200 tubular cross-sections per animal. Quantification was performed by two investigators with no knowledge of the groups.

Table 2. Effects of SPX on serum cystatin C level and SBP

	Standard-sham	Standard-SPX
Serum cystatin C level (ng/mL)	1.18 ± 0.11	1.98 ± 0.14*
SBP (mmHg)	101.4 ± 2.8	108.7 ± 1.6*

*$P < 0.05$ versus standard-sham group. Treatment groups: standard-sham, fed a standard chow and given a sham operation ($n = 6$); standard-SPX, fed a standard chow and given an SPX ($n = 6$).

For nephrin and desmin protein staining, 5-μm-thick kidney sections were incubated overnight at 4°C with goat anti-mouse nephrin (R&D System Inc., Minneapolis, MN, USA) or rabbit anti-mouse desmin (LifeSpan Biosciences, Inc., Seattle, WA, USA) and then incubated with biotin-conjugated rabbit anti-goat IgG or goat anti-rabbit IgG (ABC reagent, Vector Laboratories). Samples were visualized with rhodamine-conjugated or fluorescein isothiocyanate-conjugated streptavidin. Additionally, normal goat or rabbit serum was used instead of the aforementioned antibodies, and further incubation with a secondary antibody was performed as a negative control, which resulted in no staining.

Glomerular mesangial proliferation

Mesangial cells were counted on 10 arbitrarily selected glomeruli on PAS-stained kidney sections. Glomeruli with a diameter of 100–150 μm were evaluated.

Fibrosis in the kidney

Kidney sections were subjected to Mallory-Azan staining. The mean fibrotic area, indicated by a blue color after Mallory-Azan staining, in 10 glomerular areas per animal was

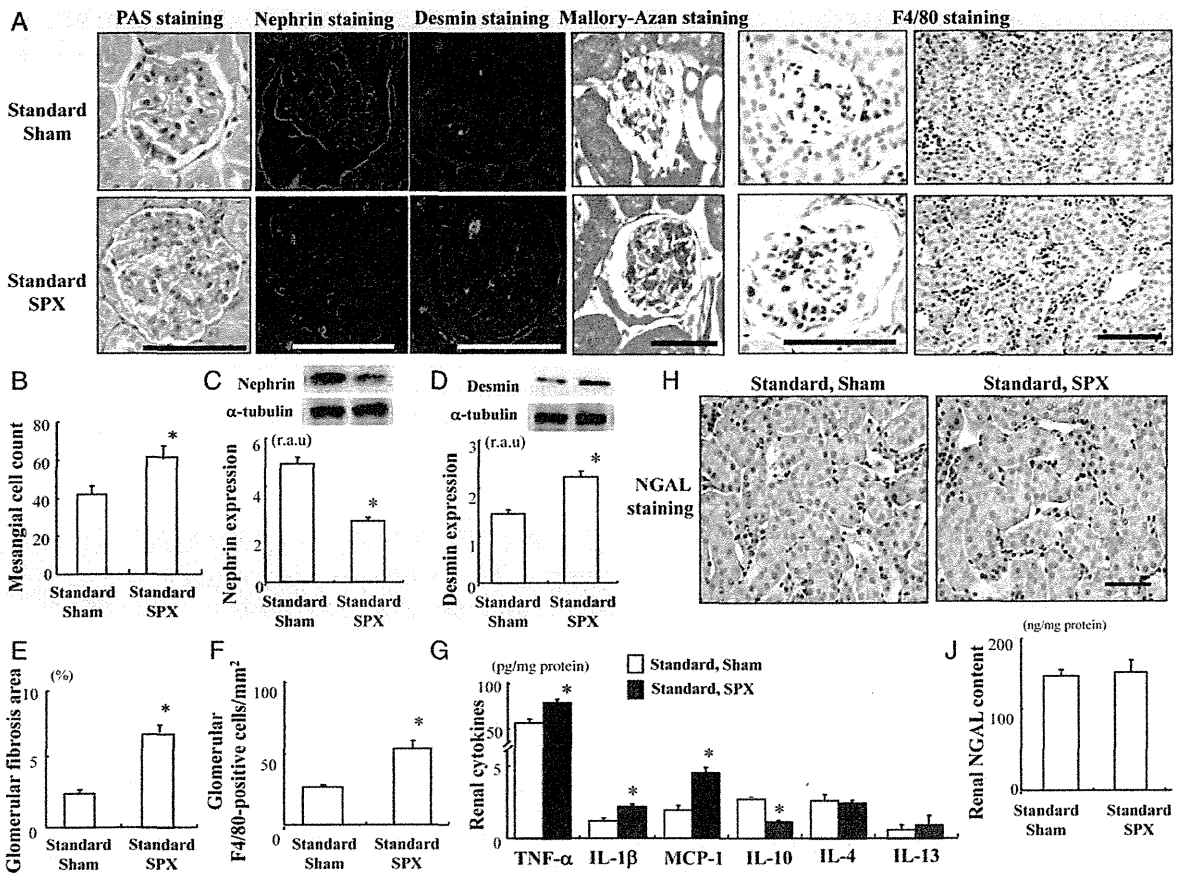

FIGURE 1: Effects of SPX on renal injury and fat accumulation in the kidney. (A) Representative PAS, nephrin, desmin, Mallory-Azan and F4/80 staining performed on kidney sections from each group. (B–G) Expansion of mesangial cell area (B), nephrin expression (C), desmin expression (D) and glomerular fibrosis area (E), glomerular F4/80-positive cells (F), renal pro- and anti-inflammatory cytokines content (G) from each group ($n = 6$). (H and I) Representative NGAL staining in kidneys (H) and renal NGAL content (I) from each group ($n = 6$). *P < 0.05 versus standard-sham group. Scale bar = 100 μm. Treatment groups: standard-sham, fed a standard chow and given a sham operation; standard-SPX, fed a standard chow and given an SPX.

evaluated as a percentage of the field using Mac Scope version 6.02 (Mitani Shoji, Fukui, Japan).

Serum cystatin C level

The serum cystatin C level was measured with a cystatin C ELISA kit (Quantikine, R&D System Inc.).

Measurement of systolic blood pressure

Systolic blood pressure (SBP) was measured in conscious mice by the tail-cuff method (Softron, Tokyo, Japan). On each day of SBP determination, 10 measurements were obtained and averaged for each mouse.

Statistics

Results were expressed as mean ± standard error of the mean. Statistical tests included two-tailed Student's *t*-test and two-way analysis of variance followed by Scheffe's test for *post hoc* comparison. For all tests, the level of significance was set at $P < 0.05$.

RESULTS

HF feeding decreases serum levels of IL-10, but not IL-1β or MCP-1

Even though pro-inflammatory (TNF-α, IL-1β and MCP-1) and anti-inflammatory (IL-4, IL-10 and IL-13) cytokine expression in the spleen was significantly lower, the serum level of only IL-10 was significantly lower in the HF group compared with the standard group (Table 1). When splenic cytokine expression was downregulated by HF feeding, the serum cytokine levels, except IL-10, were probably maintained by organs other than the spleen. However, the low serum IL-10 levels suggest that large amounts of serum IL-10 are derived from the spleen.

SPX causes renal dysfunction and elevates SBP

We investigated whether SPX contributes to renal function and SBP. SPX treatment elevated serum cystatin C levels and SBP, compared with sham treatment (Table 2).

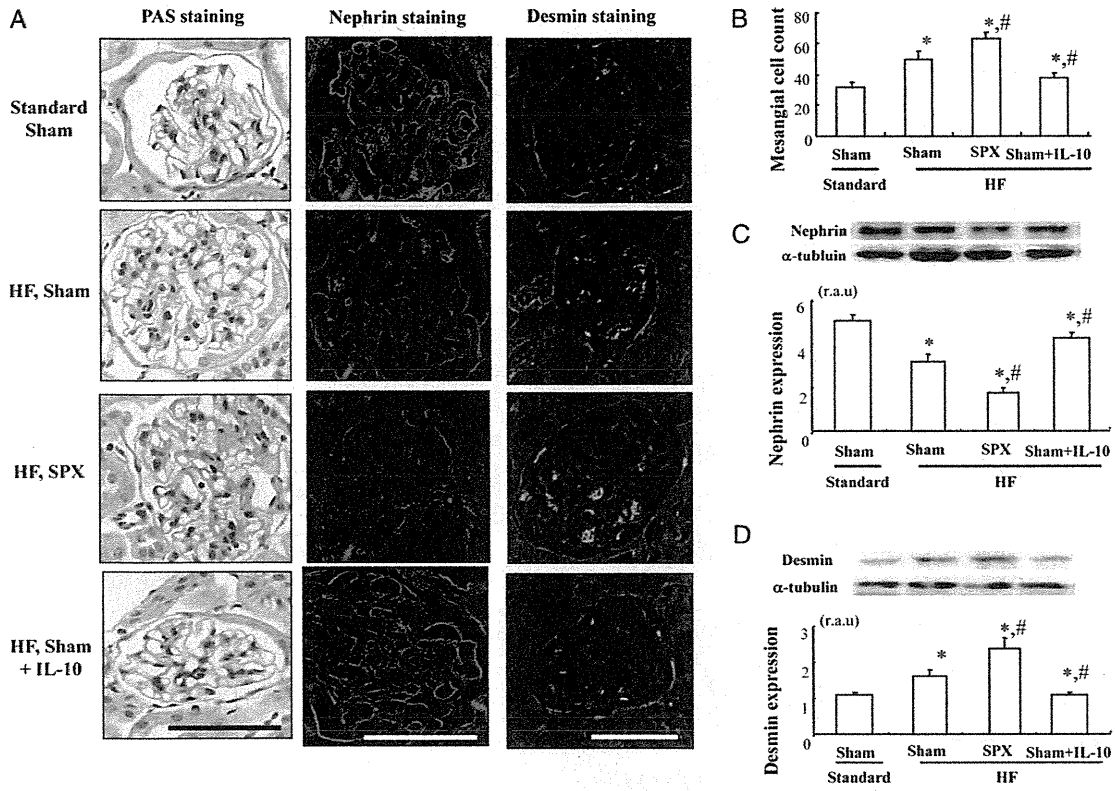

FIGURE 2: The systemic administration of IL-10 suppresses HF-induced renal damage. (A) Representative PAS staining (left row), nephrin staining (middle row) and desmin staining (right row) in the glomerular area of kidney sections from each group. Scale bar = 100 μm. (B–D) Expansion of the mesangial area (B), nephrin expression (C) and desmin expression (D) in kidneys from each group ($n = 6$). *$P < 0.05$ versus standard-sham group, #$P < 0.05$ versus HF-sham group. Treatment groups: standard-sham, fed a standard chow, administered serum albumin and given a sham operation; HF-sham, fed a HF, administered serum albumin and given a sham operation; HF-SPX, fed a HF, administered serum albumin and given an SPX, HF-sham + IL-10, fed a HF, administered IL-10 and given a sham operation.

SPX accelerates renal damage and promotes inflammation in the kidney. Next, we investigated whether SPX resulted in inflammation in the kidney. The PAS-stained renal pictures obtained in each group are shown in Figure 1A. Histological examination of the kidney revealed glomerular hypertrophy and expansion of the mesangial area in the SPX group compared with the sham group (Figure 1A and B). To examine renal injury, due to SPX, nephrin and desmin expression were evaluated qualitatively by immunofluorescence in kidney sections from each group (Figure 1A) and quantitatively by western blot (Figure 1C and D). SPX treatment significantly reduced glomerular nephrin expression and elevated desmin expression compared with sham treatment. Glomerular fibrosis was greater in the SPX group than in the sham-treated group (Figure 1A and E). Moreover, we examined the staining of kidney tissues for F4/80 in each group to evaluate changes in macrophage infiltration after SPX. The macrophage marker F4/80 staining level in glomerular and tubulointerstitial areas was increased (Figure 1A and F) in the SPX-treated group compared with the sham-treated group. Furthermore, SPX also increased pro-inflammatory cytokines such as TNF-α, IL-1β and MCP-1, but decreased anti-inflammatory cytokine, IL-10 levels, but not IL-4 and IL-13 (Figure 1G) in the kidney compared with sham treatment. We measured NGAL protein levels in the kidneys, but there was no difference between sham and SPX groups (Figure 1H and I).

IL-10 treatment inhibits the HF-induced glomerular injury

The effect of IL-10 on the HF-induced alterations in glomeruli was examined. Compared with standard feeding, HF feeding induced glomerular hypertrophy and hyperplasia of mesangial cells (Figure 2A and B) and led to decreased nephrin (Figure 2A and C) and increased desmin (Figure 2A and D) expression, suggesting that HF feeding induces renal injury. These alterations were promoted in the HF-fed SPX group to a significantly greater degree than in the HF-fed sham group (Figure 2). However, IL-10 treatment attenuated the progression of glomerular fibrosis and the alterations of nephrin and desmin expression induced by HF feeding (Figure 2).

IL-10 treatment diminishes HF-induced macrophage infiltration and fibrosis in the glomerulus, and also attenuates elevation of SBP

Interestingly, compared with standard feeding, HF feeding promoted F4/80-positive cell infiltration in glomerular as well as tubulointerstitial areas (Figure 3A and B) and fibrosis in

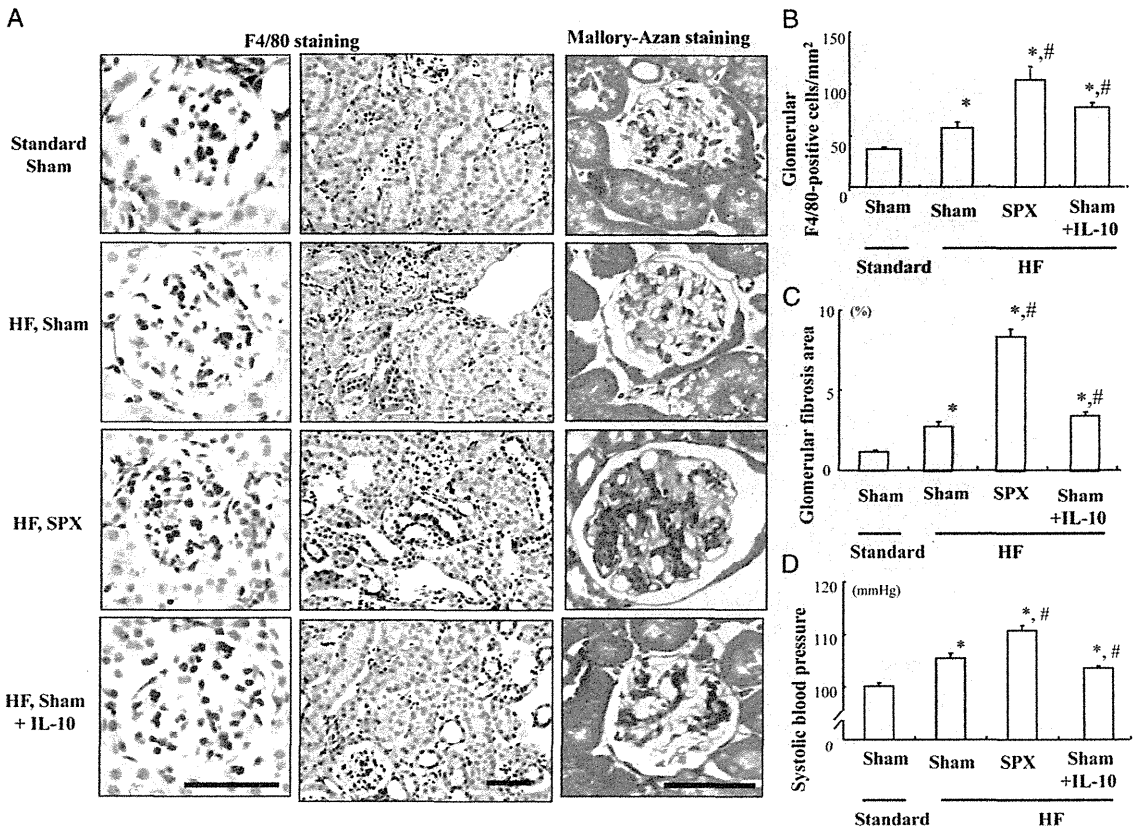

FIGURE 3: The systemic administration of IL-10 inhibits HF-induced macrophage infiltration, glomerular fibrosis and hypertension. (A) Representative F4/80 staining (left row, glomerulus; middle row, tubulointerstitial area) and Mallory-Azan staining (right row) of kidney sections from each group. Scale bar = 100 μm. (B–D) Glomerular F4/80-positive cells (B), glomerular fibrosis area (C) and SBP (D) in each group ($n = 6$). *$P < 0.05$ versus standard-sham group, #$P < 0.05$ versus HF-sham group. Treatment groups: standard-sham, fed a standard chow, administered serum albumin and given a sham operation; HF-sham, fed a HF, administered serum albumin and given a sham operation; HF-SPX, fed a HF, administered serum albumin and given an SPX; HF-sham + IL-10, fed a HF, administered IL-10 and given a sham operation.

glomeruli (Figure 3A and C) and increased SBP (Figure 3D). SPX treatment further aggravated these alterations induced by HF feeding, and IL-10 treatment suppressed HF-induced changes in inflammatory responses and blood pressure (Figure 3).

SPX alters the expression of pro- and anti-inflammatory cytokines in the kidney, elevates serum cystatin C levels and reduces the level of serum IL-10 more than the levels of other pro-inflammatory cytokines

HF feeding increased pro-inflammatory and decreased anti-inflammatory cytokine levels except IL-4 and IL-13 in the kidney, compared with standard feeding (Figure 4A). In addition, serum cystatin C levels were higher in HF feeding, compared with standard feeding (Figure 4B). Furthermore, SPX accelerated these HF-induced changes, and IL-10 treatment suppressed the HF-induced alterations (Figure 4A and B). On the other hand, there was no significant difference in the renal NGAL level in all groups (Figure 4C and D). To clarify whether spleen-derived IL-10 is more relevant to inflammation than IL-10 produced locally in the kidney, we examined serum cytokine levels in the sham and SPX groups on standard and HF feeding. SPX decreased both pro- and anti-inflammatory cytokine levels in the serum, irrespective of standard or HF feeding (Figure 4E). However, SPX reduced the serum IL-10 level by approximately 60% in mice on standard and HF feeding, and the ratio of the decrease in IL-10 by SPX was greater than that of pro-inflammatory cytokines in mice on both standard and HF feeding (Figure 4F).

SPX does not cause glomerular hypertrophy and injury in the IL-10-deficient mice

The proliferation of mesangial cells and renal injury were greater in IL-10KO mice than in wild-type mice (Figure 5). SPX promoted hyperplasia of mesangial cells (Figure 5A and B) and renal injury (Figure 5A, C and D), compared with sham treatment in wild-type mice. On the other hand, these alterations were not found in IL-10KO mice (Figure 5). However, IL-10 treatment improved these alterations in both wild-type and IL-10KO mice.

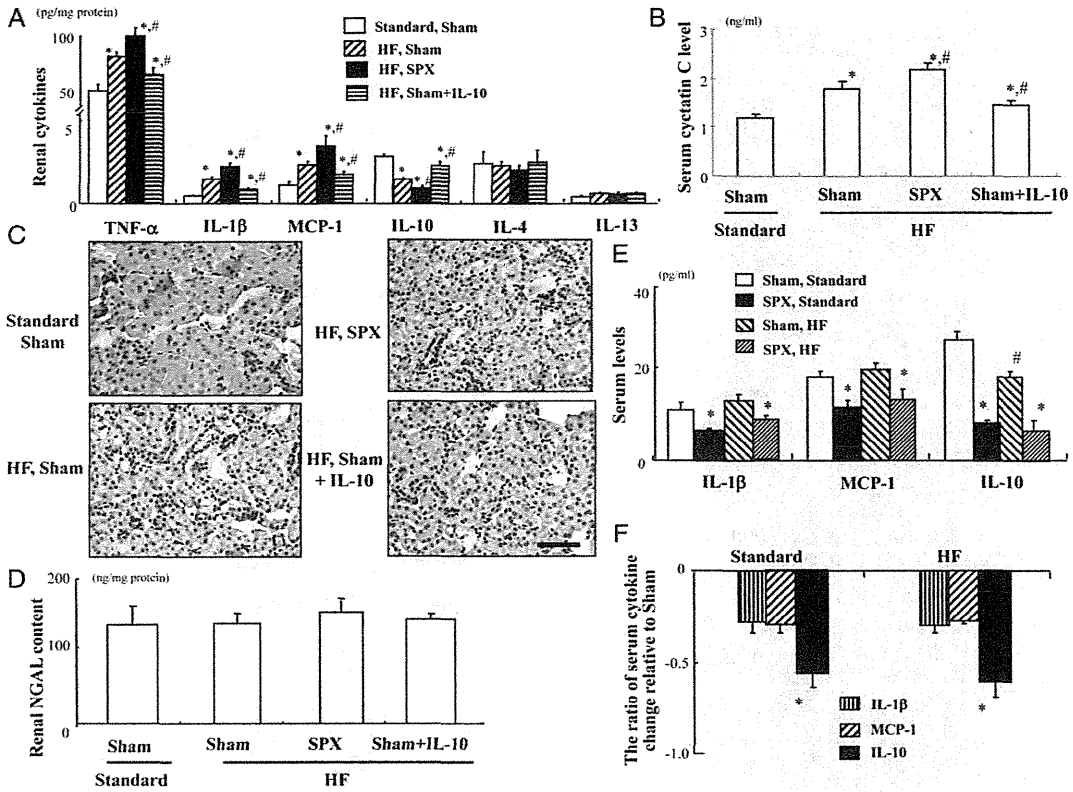

FIGURE 4: SPX alters the expression of pro- and anti-inflammatory cytokines in the kidney and reduces the level of serum IL-10 more than the levels of other pro-inflammatory cytokines. (A) Pro- and anti-inflammatory cytokines content in the kidneys of each group ($n = 6$). (B) Serum cystatin C levels in each group. *$P < 0.05$ versus standard-sham group, #$P < 0.05$ versus HF-sham group. (C and D) Representative NGAL staining (C) and renal NGAL level (D) in each group ($n = 6$). (E) Serum levels of IL-1β, MCP-1 and IL-10 in the sham and SPX groups on standard and HF feeding ($n = 6$ in each). *$P < 0.05$ versus standard-sham group and HF-sham group, #$P < 0.05$ versus standard-sham group. (F) Ratio of serum cytokine change relative to the standard-sham group ($n = 6$, in each). *$P < 0.05$ versus IL-1β and MCP-1. Treatment groups: standard-sham, fed a standard chow, administered serum albumin and given a sham operation; HF-sham, fed a HF, administered serum albumin and given a sham operation; HF-SPX, fed a HF, administered serum albumin and given an SPX; HF-sham + IL-10, fed a HF, administered IL-10 and given a sham operation.

SPX does not affect renal injury, including fibrosis, SBP or serum cystatin C levels in the kidneys of IL-10-deficient mice

The infiltration of F4/80-positive cells and glomerular fibrosis were greater in IL-10KO mice than in wild-type mice. SPX resulted in acceleration of F4/80-positive cell infiltration and fibrosis in the glomeruli, compared with sham treatment in wild-type mice (Figure 6A and B). However, these observations were not seen in IL-10KO mice. Furthermore, SPX-induced glomerular macrophage infiltration and fibrosis (Figure 6A and C), elevation of SBP and serum cystatin C level (Figure 6D and E) observed in wild-type mice were also not found in IL-10KO mice. Meanwhile, IL-10 treatment improved these alterations in both wild-type and IL-10KO mice (Figure 6).

SPX has no effect on pro-inflammatory responses in IL-10-deficient mice

SPX-induced acceleration of F4/80-positive cells in tubulointerstitial areas and increase of renal pro-inflammatory cytokine contents were not observed in IL-10KO mice (Figure 7A and B). Furthermore, IL-10 treatment also improved these alterations in both mice (Figure 7A and B). However, there was no difference in renal IL-4, IL-13 and NGAL levels among all groups (Figure 7B and D).

DISCUSSION

Obesity is associated with a low-grade, chronic, pro-inflammatory condition [12, 13]. However, the primary cause of obesity-induced inflammation is not well understood. Our previous study revealed that SPX aggravated obesity-induced inflammatory responses such as elevation of pro-inflammatory cytokines (TNF-α, IL-1β and MCP-1) and infiltration of F4/80-positive cells in the liver of wild-type mice, but not of IL-10KO mice [14]. This is the first study to systematically characterize the effect of a lack of IL-10 production in the spleen due to HF-induced obesity and SPX in mice, with respect to the kidney.

IL-10 is synthesized by several cell types in multiple organs, including the spleen. We noted spleen-derived IL-10 because

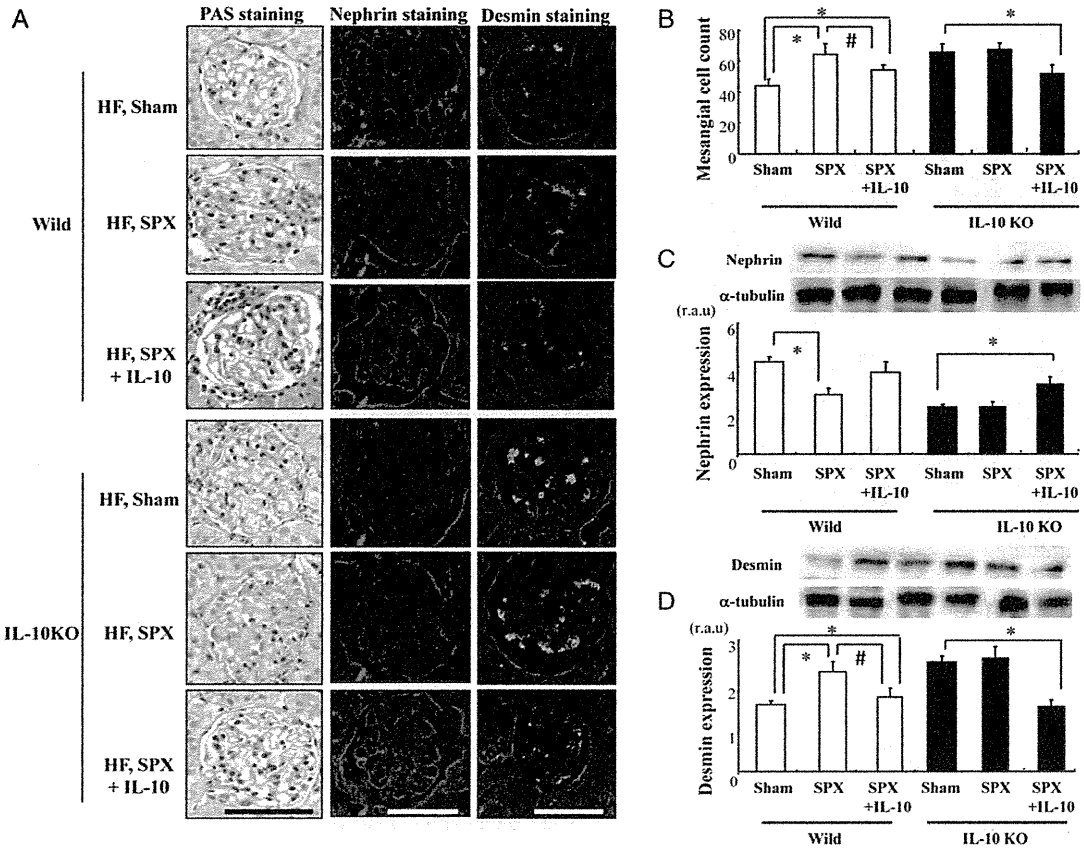

FIGURE 5: SPX has little effect on renal damage in IL-10-deficient mice. (A) Representative PAS staining (left row), nephrin staining (middle row) and desmin staining (right row) in the glomerular area of kidney sections from each group ($n = 6$). Scale bar = 100 μm. (B–D) Expansion of mesangial area (B), nephrin expression (C) and desmin expression (D) in kidneys of each group ($n = 6$). *P < 0.05 versus sham (wild-type or IL-10KO) group, #P < 0.05 versus SPX (wild-type) group. Treatment groups: sham, fed a HF, administered serum albumin and given a sham operation; SPX, fed a HF, administered serum albumin and given an SPX; SPX + IL-10, fed a HF, administered r-IL-10 and given an SPX; Wild-type, wild-type mice; IL-10KO, IL-10-deficient mice.

the serum level of only IL-10, despite the significantly decreased expression of all cytokines in the spleens of HF-fed mice compared with standard-fed mice. This suggested that large amounts of serum IL-10 are derived from the spleen and that obesity reduces IL-10 secretion from the spleen. Our previous research showed that HF feeding compared with standard feeding, downregulated the expression of CD20, a surface molecule present on B cells, which play a large role in the immune response and produce IL-10 mainly in the spleen [15]. Moreover, splenocyte proliferation stimulated by T-cell and B-cell mitogens was significantly lower in obese subjects; thus, the functions of both T-cells and B-cells in the spleen may be impaired in obesity [16]. We hypothesized that the obesity-induced reduction in IL-10 synthesis in the spleen could lead to inflammatory responses in the kidneys and to metabolic disorders.

It is known that podocyte loss and dysfunction occur as the magnitude of glomerulosclerosis increases. Because podocytes serve as the final barrier against urinary loss in normal glomeruli, any change in podocyte structure or function may be intimately associated with proteinuria and consequent glomerular sclerosis [17]. It is possible that the loss of podocyte nephrin is the transition step from an obesity-related glomerular change to the pathogenesis of proteinuria [18]. Our data suggest that the obesity-induced reduction of nephrin expression was markedly accelerated by SPX and that IL-10 administration to HF-fed mice elevated nephrin expression to a level comparable with that in standard-fed mice. We also found that the obesity-induced increase in desmin, an intermediate filament protein and a specific and sensitive podocyte injury marker, was elevated in the glomeruli after SPX. However, HF-induced increase in desmin expression in the glomeruli was attenuated by IL-10 administration. Furthermore, the alterations of glomerular hypertrophy, fibrosis and hyperplasia of mesangial cells, SBP and serum cystatin C level that reflects severe renal damage were similar in all groups [19, 20]. These results would support our assertion that splenic IL-10 production is necessary to downregulate HF-induced pro-inflammatory response to renal damage.

To further clarify the influence of spleen-derived IL-10 in protection against inflammation in the kidney induced by SPX treatment, we examined whether IL-10 deficiency affected SPX-induced alterations in the kidneys using IL-10KO mice. The SPX-induced pro-inflammatory effects, acceleration of

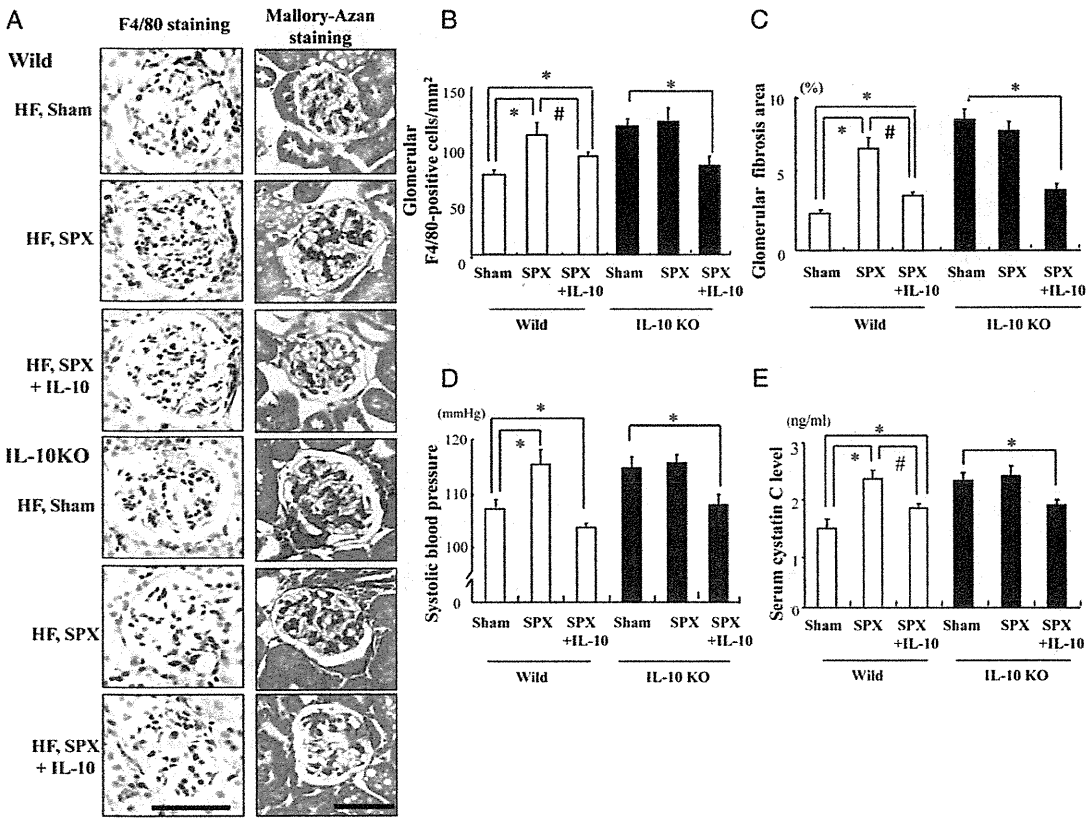

FIGURE 6: SPX has little effect on macrophage infiltration and fibrosis in glomerulus, and pro-inflammatory responses in the kidneys of IL-10-deficient mice. (**A**) Representative F4/80 staining (left row) and Mallory-Azan staining (right row) in the glomerular area of kidney sections from each group. Scale bar = 100 μm. (**B–E**) F4/80-positive cells (B), glomerular fibrosis area (C), SBP (D) and serum cystatin C levels (E) in each group ($n = 6$). *$P < 0.05$ versus sham (wild-type or IL-10KO) group, #$P < 0.05$ versus SPX (wild-type) group. Treatment groups: sham, fed a HF, administered serum albumin and given a sham operation; SPX, fed a HF, administered serum albumin and given an SPX; SPX + IL-10, fed a HF, administered r-IL-10 and given an SPX; Wild, wild-type mice; IL-10KO, IL-10-deficient mice.

hypertrophy and fibrosis in glomeruli, decrease of nephrin, increase of desmin expression in the kidneys and elevation of SBP as well as serum cystatin C levels observed in wild-type mice were not seen in IL-10KO mice. However, IL-10 treatment restored these alterations in the kidney in SPX-treated wild-type mice and IL-10KO mice. These results support the view that the obesity-induced reduction of spleen-derived IL-10 may result in renal damage. NGAL also has great promise as a biomarker of CKD including diabetic nephropathy [21, 22]. However, in this research, renal NGAL levels were not increased in the absence of spleen-derived IL-10, supporting the other study showing there is no difference in the whole kidney of streptozotocin (STZ) as a model of slowly progressive CKD and non-STZ mice. We suggest that NGAL might be useful as a marker of acute worsening of CKD because other research propose that induction of NGAL expression is a real-time indicator of acute renal injury [23]. Taken together, these data suggest that IL-10 originating in the spleen may prevent obesity-induced CKD.

In chronic inflammatory conditions, defective IL-10 synthesis contributes to increased pro-inflammatory cytokine levels [24]. We examined serum cytokine levels in the sham and SPX groups on standard and HF feeding. We found that the serum IL-10 level was reduced by more than half by SPX in mice on both standard and HF feeding, which induces a strong systemic inflammatory response. Simultaneously, SPX treatment also decreased the expression of IL-10 locally in the kidneys. In contrast, we also observed that SPX induced a maximum 40% decrease in serum pro-inflammatory cytokine levels, suggesting that pro-inflammatory cytokines are predominantly produced in other organs except the spleen, rather than anti-inflammatory cytokines such as IL-10, although both pro- and anti-inflammatory cytokines are produced in the spleen [8, 9]. Indeed, SPX eliminates both pro- and anti-inflammatory cytokine productions by the spleen. However, because SPX did not affect fat accumulation and inflammatory responses in the kidneys of IL-10-deficient mice, the SPX-induced alterations observed in the kidneys of wild-type mice were likely not due to the elimination of pro-inflammatory cytokines after SPX.

Macrophage infiltration in the kidney has an important role in the development and progression of renal diseases. HF feeding triggers the recruitment of macrophages, which release pro-inflammatory cytokines causing metabolic disorders including CKD [25]. Moreover, the balance between pro-inflammatory and anti-inflammatory cytokines determines the